ORIGINAL PAPER

Sources and mixing of sulfate contamination in the water environment of a typical coal mining city, China: evidence from stable isotope characteristics

Xing Chen · Liugen Zheng · Xianglin Dong · Chunlu Jiang · Xiangping Wei

Abstract To explore the sources and distribution characteristics of SO_4^{2-} in the surface waters of the Linhuan mining area in Huaibei, river and surface water samples in subsidence and mine drainage locations in the study area were collected at different times. The conventional hydrochemical indexes and the eigenvalues of sulfur and oxygen isotopes were tested and analyzed. The results suggested the following: (1) The SO_4^{2-} content showed seasonal changes: low-flow seasons > mid-flow seasons > high-flow seasons. (2) Based on $\delta^{34}S_{SO4}$ and $\delta^{18}O_{SO4}$ isotope analyses, the main source of SO_4^{2-} was the dissolution of evaporite salt rocks in the stratum of the upstream area. The SO_4^{2-} in the subsidence area was mainly from the river water supply, mine drainage and coal gangue leaching. The high concentration of SO_4^{2-} in the mine drainage was mainly from the dissolution of evaporative salt rocks. (3) The calculation results of the ternary mixing model showed that the SO_4^{2-} in the subsidence area water was affected by mine drainage and gangue leaching to different degrees. The results showed that the sulfate contribution proportion of the river water source to the subsidence area water was 35.8–65.9%; the sulfate contribution proportion of the mine drainage source to the subsidence area water was 2.0–26.6%; and the sulfate contribution proportion of the gangue leaching end source ranged from 16.3% to 56.9%. Coal mining activities had an important impact on the sulfate in the subsidence area water.

Keywords Sulfate contamination · Isotope characteristics · Mixed model · Source terminal

X. Chen · L. Zheng (✉) · C. Jiang
Collaborative Innovation Center for Mines Environmental Remediation and Wetland Ecological Security, School of Resource and Environment Engineering, Anhui University, 111 Jiulong Road, Hefei 230601, Anhui Province, China
e-mail: lgzheng@ustc.edu.cn

Present Address:
X. Chen · L. Zheng · C. Jiang
Anhui Province Engineering Laboratory for Mine Ecological Remediation, Hefei, China

X. Dong · X. Wei
Geological Survey Division, Huaibei Coal Mining Group Corporation, Huaibei 235001, China
e-mail: 15705610332@163.com

Introduction

Coal has always been the main energy resource consumed in China. With increasing coal consumption, coal mining activities are increasingly intensified. Large-scale and high-intensity coal mining activities lead to formation damage and large amounts of water accumulation. Large-scale subsidence caused by mining activities has formed a wide range of subsidence water. Subsidence areas and the surrounding rivers and groundwater play an important role in

maintaining ecological balance (Chen et al. 2011, 2019; Lu et al. 2017a, b; Liu et al. 2009). For example, 14 mining areas will be part of the subsidence area in Huaibei by 2020. The subsidence area will be divided into five water accumulation areas, namely East Lake, South Lake, West Lake, Linhaitong Lake and Shuoli Lake. By that time, the effective storage capacity of the water will reach 132 million m^3 (Zhang et al. 2014, 2015; Xie et al. 2013). With the development of the coal industry, water pollution in the subsidence area will become increasingly serious. Some scholars have carried out a large number of studies on water environment problems in the subsidence areas (Chen et al. 2019; Fang et al. 2015; Hu et al. 2017; Han and Zhang 2017; Wei et al. 2016; Yi et al. 2015; Wang et al. 2015; Liu et al. 2009; Wang et al. 2009). However, these studies have mainly focused on nitrogen, phosphorus and heavy metals pollutions in the water bodies and have paid little attention to sulfate pollution. Soluble sulfate is an important component of surface water, and SO_4^{2-} participates in the weathering process of carbonate rocks, which is closely related to the release of CO_2 in the atmosphere, thus affecting the global carbon cycle. On the other hand, excessive sulfate will seriously affect water quality, by increasing the salinity and acidifying water bodies (Cao et al. 2018; Li et al. 2013, 2015; Balci et al. 2012; Calmels et al. 2007). As the main water source for production and lives of the residents surrounding the mining area, the water in the subsidence area will cause harm to the ecological environment and the physical health of the residents. Therefore, determining and controlling specific sources of sulfate are particularly important.

Sulfate can often be found in surface water, and its sources mainly include natural (rock dissolution, sulfide mineral oxidation, atmospheric deposition, etc.) and artificial (industrial and agricultural sewage, fertilizer, mining wastewater, etc.) sources (Li et al. 2013; Balci et al. 2007, 2012; Choi et al. 2011; Otero et al. 2008; Torssander et al. 2006; Dogramaci et al. 2001). With the increasing impact of human activities, it is impossible to accurately distinguish the source of components in water based on hydrochemical composition and traditional ion source identification methods. The use of sulfur and oxygen isotopes can more accurately trace the sources of sulfate, and the contribution proportion of each pollution end source can be quantified. Sulfur isotope fractionation widely

exists in chemical and biochemical processes, and chemical reactions are common in the process of sulfate mineral precipitation and dissolution. The kinetic isotope fractionation effect of such reactions is small; for example, the dissolution of gypsum does not produce relatively more obvious SO_4^{2-} isotope fractionation. Similarly, in addition to the reduction in sulfate bacteria, sulfur isotope and oxygen isotope fractionation in the adsorption process of SO_4^{2-} is only -0.3‰ and 0.1‰, respectively. The isotopic composition of sulfates from different sources differs, and those differences are reflected in the eigenvalues of the isotope (Li et al. 2013; Nriagu et al. 1991). In most cases, the isotopic composition of SO_4^{2-} can be used to trace its origin. $\delta^{34}S_{SO4}$ and $\delta^{18}O_{SO4}$ can be used to distinguish natural and anthropogenic sulfates. Therefore, isotopes can be used as an effective way to trace the source of sulfate in the surface water of mining areas.

The isotopes to trace sulfate sources in water have been used extensively. Sulfur isotopes in river systems have been studied worldwide since the 1960s. Since then, a series of studies on sulfur isotopes in surface water, such as rivers, have been carried out in China. However, the domestic and foreign studies on this aspect have mainly focused on the source and circulation of sulfate at the scale of large rivers. Some scholars conducted isotope tracing studies on sulfate sources in the Yangtze River, Heihe River and Yellow River (Li et al. 2013; Zhang et al. 2013), respectively. The sulfate in the Yangtze River and Heihe River mainly originated from the oxidation of sulfide minerals and acid rain. In the mainstream of the Yellow River, the sulfate originated from sulfate dissolution in soil and gypsum dissolution. Few researchers have studied the sources of high amounts of sulfate in the surface water of subsidence areas combined with coal mining areas. The water storage situation of mining subsidence is complex, and excessive gangue accumulation and coal mining activities result in severe sulfate pollution; however, the specific source and proportions remain unclear. Therefore, the hydrochemical composition and isotopic composition of the surface water in the Linhuan mining area of Huaibei were the basis for this research. Combining the data with local geological and climatic conditions, the variation characteristics of the SO_4^{2-} content in the surface water were analyzed and source analysis and the quantification of pollution end

sources in the subsidence water area were conducted. By analyzing the surface water samples collected in different seasons, the seasonal variation characteristics of the main ions were analyzed. The effects of climate, geological factors and human activities on the chemical composition characteristics of the surface water in the study area were distinguished and evaluated. At the same time, data and a scientific basis were provided for the rational development, management and utilization of water resources and the evaluation of water quality in mining areas.

Survey of the research area

The Linhuan mining area is located southwest of Huaibei city, Anhui Province. The area is approximately 40.0 km north of Huaibei city and 30.0 km east of Suzhou city. The climate belongs to the north temperate zone, which is mild and sunny, year-round. There are four distinct seasons and with the average annual temperature of 14.5 °C. The average annual precipitation is 830 mm, the average annual evaporation is 1213.6 mm, there are approximately 2315.8 h of annual sunshine on average, and the dominant wind direction is southeast in summer and northeast in winter. Generally, the freezing period is from early December to mid-February, and the maximum depth of frozen soil can reach 19.0 cm. The vegetation in the Linhuan coal mine is mainly terrestrial. The main crop types include wheat, soybean, corn, sesame, vegetables, melons and fruits. The main soil types in the region are tidal, silt black, mortar black and green loess (Fan et al. 2017; Lu et al. 2017a, b).

Linhuan is located on the Huaibei Plain, and the terrain is flat and open. The elevation ranges from + 20.78 to + 28.58 m, and the average is approximately + 27.0 m, which is high in the northwest and low in the southeast. The mining stratum is subordinate to the Huaihe River stratigraphic division of the Huaihe River strata in the Jinji-Luyu stratigraphic zone of the North China strata. The coal-bearing strata in the area are concealed under loose stratum of the Cenozoic. The study area is surrounded by four major faults: Nanping fault to the east, Fengwo fault to the west, Subei fault to the north and Banqiao fault to the south. Its hydrogeological conditions are limited by the surrounding large faults, forming a grid-like hydrogeological unit with a total coverage of 892

km^2. This area belongs to the concealed mining area, with flat terrain, igneous rock intrusion in the area and complex structure. The strata in the area are Ordovician, Carboniferous, Permian, Tertiary and Quaternary from the bottom to the top.

A river passing through the study area and water from the coal mining subsidence area are the main surface waters. The Huihe River is the main transit river, and the surface water in the subsidence area is concentrated north of Linhuan coal mine industrial park, which is located south of the Huihe River and west of Hancun town. According to the relationship between the subsidence area and the surface river, the subsidence division is divided into two types; the first type is closed subsidence area. It only has surface runoff flow from the surface, the pollution type is non-point source pollution, and the subsidence area water has a certain hydraulic relationship with groundwater. The second type is open subsidence area, connected to the surrounding surface water. In addition to the runoff replenishment from the surrounding ditches, there are rivers or lakes passing through, and water flowing into and out of the river. The mining subsidence area in Linhuan coal mine is an open subsidence area, the ditch which connected with the Huihe River is the only way to introduce the river water as its water source supply, and the river water is a replenishment relationship to the water in the subsidence area. The main source of the subsidence area water loss is evaporation, with an average water depth of 3.45 m and a maximum water depth of 9.0 m. According to lithology, burial conditions and water-bearing characteristics, the aquifers in Linhuan mining area can be divided into three types from top to bottom. The first is a loose porous aquifer formed by the loose alternating deposition of sand and clay. The second is the fractured coal and sandstone strata, which are composed of sandstone layers and siltstone layers, including quartz, feldspar, mica, gypsum and other minerals, including three groups of related coal beds, 7–8 coal beds and ten coal beds. The last is the deeply buried karst aquifer. The deeply buried karst aquifer formed by Carboniferous limestone in Taiyuan formation is Ordovician limestone and Cambrian limestone, which is a relatively uniform groundwater flow system. The coal mining subsidence area is approximately 3.7546×10^6 m^2. The bottom of the subsidence area is composed of clay and sandy clay. The groundwater level elevation is 22.6–25.8 m. Moreover, the

groundwater hydraulic gradient is gentle, the runoff is weak, and the groundwater level difference is small. The hydraulic connection between the water table in the subsidence area and the groundwater is not obvious (Qiu et al. 2018; Lu et al. 2017a, b; Shang et al. 2016).

Sample collection and test analysis

Sample collection and pretreatment

Combined with the hydrogeological conditions of the study area and the actual situation of the site, 45 surface water samples comprising 21 subsidence area water samples and 24 river water samples were collected from the Linhuan mining area in April 2015 (mid-flow seasons), July 2015 (high-flow seasons), January 2016 (low-flow seasons) and December 2017. The samples for the isotope test were taken from the three river water samples and 12 subsidence area water samples collected in December 2017; other drainage samples from local coal mines were taken. Two precipitation samples were collected in July 2015 and January 2016. The specific distribution of sampling points is shown in Fig. 1.

Water samples were collected using precleaned 500 ml high-density polyethylene plastic bottles. The sample bottle was repeatedly washed with the original water sample 3–5 times before sampling, and the sample bottles were quickly filled during sampling to ensure that no bubbles were left in the bottles. The headspace of the bottles remained sealed, and the water samples were kept at low temperature. The latitude and longitude of the sample points, the time and the surrounding characteristics were recorded. Basic water quality parameters such as the water temperature, pH, redox potential, EC and TDS were measured in the field using a pH meter (WTW pH 3110) and a portable water quality tester (WTWoxi 315i). The water samples were filtered in the field using a 0.45-μm acetate filter and then returned to the laboratory. The water samples for cation analysis were acidified with HNO_3 to adjust the pH < 2. The water samples for anion analysis were further filtered with a 0.22 μm Millipore membrane and bottled for testing. The water samples for hydrogen and oxygen isotopes were separately dispensed and stored in a sealed container to prevent the fractional distillation of the

isotope. Another 2L water sample was acidified with dilute HCl to a pH < 2. A saturated $BaCl_2$ solution was then added, and $BaSO_4$ precipitate was generated. After standing and stratification, the resulting precipitate was filtered using a 0.45-μm cellulose acetate filter, and the $BaSO_4$ was dried at 105 °C and kept in a desiccator. The treated $BaSO_4$ precipitate was dissolved and re-precipitated by the DDARP method, and the $BaSO_4$ was then dissolved in a diethylenetriamine-pentaacetic acid (DTPA) alkali solution [0.05 M DTPA + 1 M NaOH]. The completely dissolved solution of $BaSO_4$ was filtered through a 0.22-μm filter, and several drops of 10 M HCl were added to the solution. The pH was adjusted to 3–4, and the $BaSO_4$ was then precipitated again. Finally, the precipitate was washed three times with deionized water and dried prior to further analysis (Bao 2006).

Analytical methods

Water samples of cation and anion were tested in the engineering laboratory for mine ecological remediation of Anhui University. The concentration of anions (F^-, Cl^-, SO_4^{2-}) was tested using an ion chromatograph (DIONEX, model ICS-1500). The anion is separated by an AS-14 anion exchange column. The eluent is a mixture of dilute Na_2CO_3 and $NaHCO_3$, the flow rate is set to 1 ml/min, and the injection volume is 25 μl. The working parameters of the suppressor were ASRS = 4 mm, I = 30 mA, and the working pressure was set at 0.2 MPa. The mixed standard liquid is prepared from the standard materials. The peak height is plotted on the ordinate, and the abscissa is the ion concentration to establish a standard curve. The peak height was determined, and R^2 was found to be greater than 0.999. Deionized water is used as the inhibitor and diluent. All samples were tested repeatedly for three times with a test accuracy of 0.01 mg/L. The anions were measured in accordance with the Chinese Environmental Protection Standard HJ/T 84–2001.

ICP-AES (IRIS Intrepid II XSP) was used to determine anions (K^+, Ca^{2+}, Na^+, Mg^{2+}) in water samples. The carrier gas was argon, the flow rate is 0.7 L/min, the flow rate of auxiliary gas was 1.0 L/min, and the RF power was set at 1150 W. Select different wavelengths to test their corresponding ions. Standard substances (GSB-1720, GSB-1735, GSB-1736 and GSB-1738) were derived from the national standard substance center at a concentration of 1.0 mg/L.
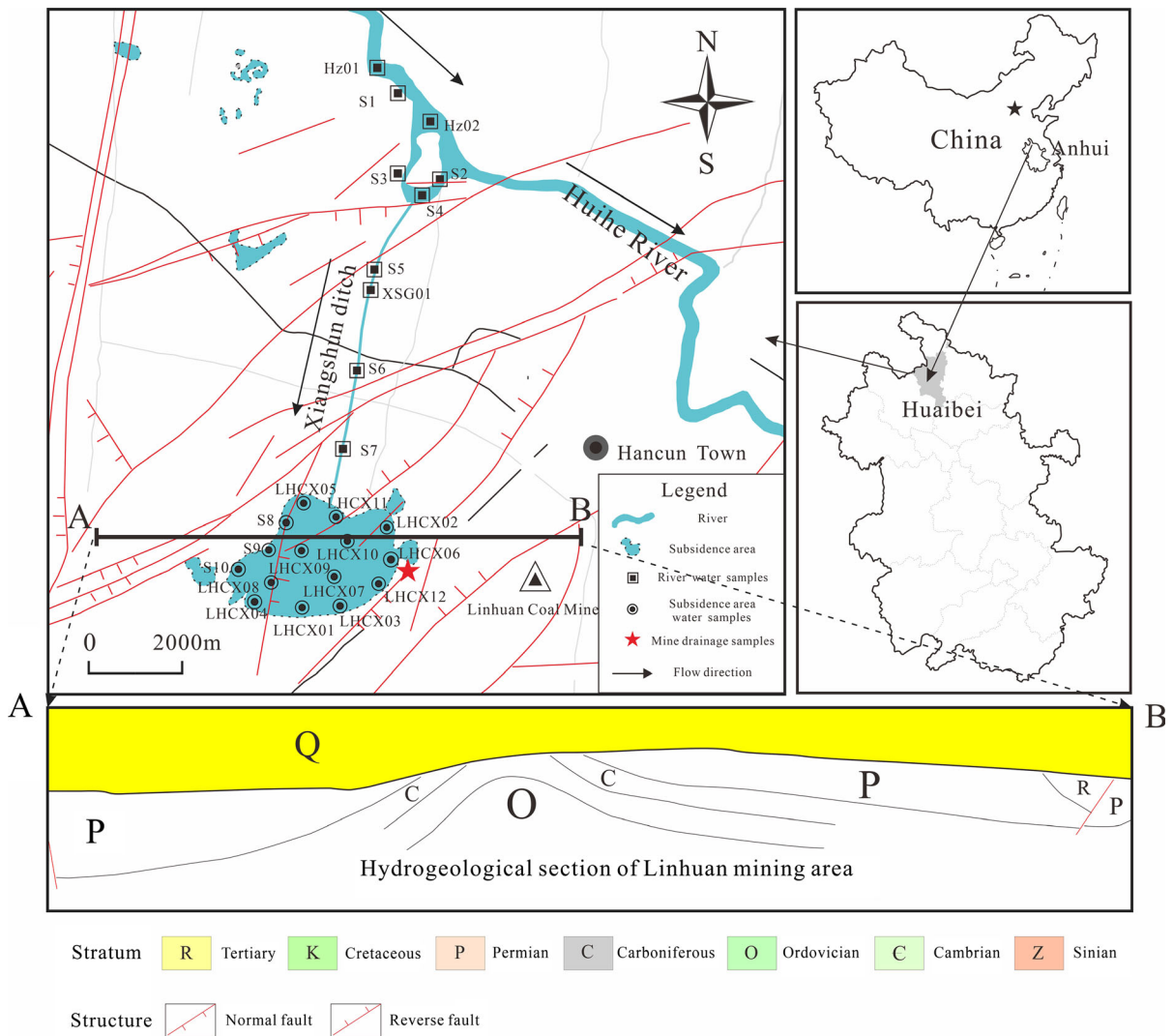
Fig. 1 Sample points of the different types of surface water in the Linhuan mining area

According to the Chinese Environmental Protection Standard HJ/776–2015, the standard recovery rate of soluble cation was 90.5–98.3%. Blank sample, duplicate sample and standard sample were used, and the sample test was repeated for three times with the test accuracy of 0.01 mg/L; ultra-pure deionized water was also used to control the accuracy of the sample determination. Double indicator titration method was used for HCO_3^- determination, with three parallel samples for each sample, and the control error was < 5%. The mass concentration of total dissolved solids (TDS) in water was calculated by subtracting 1/2 HCO_3^- mass concentration from the sum of the mass concentrations of anion and cation. The reagents used were all excellent grades. In order to ensure the accuracy of the test, the conservation of the main anion and cation was calculated. When the ratio of the equivalent concentration was in the range of 1.00 ± 0.1, the conservation of ions is considered, otherwise re-measured.

The isotopic ratio of samples was expressed as $\delta_{sample}(‰) = [(R_{sample} - R_{standard})/R_{standard}] \times 1000$. The isotopic ratios of hydrogen, oxygen and sulfur are expressed as $^2H/^1H$, $^{18}O/^{16}O$ and $^{34}S/^{32}S$. $\delta^{34}S$ and $\delta^{18}O_{SO4}$ of samples were determined in the State Key Laboratory of Biogeology and Environmental Geology of China University of Geosciences (Wuhan) by an elemental analyzer-stable isotope ratio mass

spectrometer (Thermo Fisher, Delta v Plus). When the temperature of the instrument was raised to about 1000 °C, $BaSO_4$ was burned by O_2 and V_2O_5 to produce SO_2. At this time, the $\delta^{34}S$ value in the gas was measured. The temperature of the instrument was then raised to 1300 °C and passed in C to burn BaSO4 that generated CO gas, at which time the value of $\delta^{18}O_{SO4}$ in the gas is measured. The IAEA standard materials (NBS127, IAEA-S05 and IAEA-S06) were tested together in the experiment with standard deviations < 0.25%. The internal standard was repeatedly measured. The $\delta^{18}O_{SO4}$ test accuracy is better than ± 0.3‰, and the $\delta^{34}S$ test accuracy is better than ± 0.2‰. According to the International Atomic Energy Standard Substance Correction, $\delta^{34}S$ was corrected to the VCDT international standard, and $\delta^{18}O_{SO4}$ was corrected to the VSMOW international standard. The samples were sent to the State Key Laboratory of Loess and Quaternary Geology of the Institute of Earth Environment, Chinese Academy of Sciences for δD and $\delta^{18}O$ value analysis. The experimental instrument used a laser liquid water isotope analyzer (Picarro, L2130-i type). The sample was first vaporized and attenuated in the optical cavity. The instrument automatically recorded and compared the ringing time of the cavity filled with the target gas. This time difference was the difference in the ringing time caused by the target gas absorbing the laser. The time difference is linearly related to the gas concentrations, which ensured the accuracy of δD and $\delta^{18}O$ measurements. Laboratory standard materials (SA-1, SA-3 and SA-4) and standard GISP were used in the experiments, with uncertainty better than ± 0.1‰ for $\delta^{18}O$ and better than ± 0.5‰ for δD. Experimental data were corrected to VSMOW international standards.

Data analysis

SPSS (IBM, 21.0) software was used to analyze the experimental data, including one-way analysis of variance (ANOVA), statistical analysis and correlation analysis. All the figures were drawn by the Origin 2017 software, and the experimental data are expressed as mean ± SD.

Results and discussion

Time variation characteristics of sulfate in the surface water

The mass concentration composition of the main ions in the different types of water bodies in the Linhuan mining area is shown in Table 1. The surface water in the study area showed consistent variation. The average mass concentration of ions occurred in the following order: low-flow seasons > mid-flow seasons > high-flow seasons. The order of the average mass concentration of the major cations in the surface water was $Na^+ > Ca^{2+} > Mg^{2+} > K^+$. The order of the average mass concentrations of the anions was $SO_4^{2-} > HCO_3^- > Cl^- > F^-$. In general, the contents of the cations Na^+ and Ca^{2+} in the surface water were relatively high, while HCO_3^- and SO_4^{2-} were the main anion components. The main water quality type of the surface water was $Na^+–Cl^-–SO_4^{2-}$.

The specific change trend in the average mass concentration of SO_4^{2-} in the surface water with time is shown in Fig. 2. According to a systematic sampling survey of 18 rivers by Chen et al., the average SO_4^{2-} content in the rivers of the Huaibei coalfield was 386.7 mg/L (Chen et al. 2016). From Fig. 2, the SO_4^{2-} change in the surface water was relatively large over time. The average mass concentrations were 528.4 ± 17.6, 442.7 ± 50.0, 682.8 ± 69.4 and 411.3 ± 75.3 mg/L, which all exceeded the standard limit of sulfate in drinking water (250 mg/L) based on the Environmental Quality Standard for Surface Water (GB3838-2002) and the mean value of river water in the Huaibei coalfield. The relationship between the atmospheric precipitation in the study area and time is shown in Fig. 3. The precipitation in the high-flow seasons led to a decrease in the SO_4^{2-} concentration, and for the low-flow seasons, the SO_4^{2-} concentration increased. However, the SO_4^{2-} content in the surface water during the same low-flow seasons in December 2017 was significantly lower than the previous average level. Further analysis showed that there had been in continuous rainy weather during this month, the accumulated rainfall was relatively large and significantly higher than the previous level, the evaporation was weakened, and the atmospheric precipitation had a certain dilution effect on the surface water in the research area.

Table 1 Chemical composition of the surface water and different stages in the Linhuan mining area (mg/L)

| Time		K^+	Ca^{2+}	Na^+	Mg^{2+}	SO_4^{2-}	Cl^-	HCO_3^-	TDS
2015.4	Min	12.9	87.5	233	66.4	508	150	334	1227
	Max	15.5	96.6	267	75.9	561	173	372	1376
	Mean ± SD	13.8 ± 0.7	92.4 ± 3.4	248 ± 12.5	70.7 ± 3.2	528 ± 17.6	161 ± 8.5	352 ± 11.0	1301 ± 64.56
	CV	4.84	3.72	5.02	4.59	3.32	5.29	3.14	4.96
2015.7	Min	12.3	76.5	181	70.2	389	147	331	1042
	Max	15.0	90.4	240	79.5	526	167	361	1299
	Mean ± SD	13.5 ± 1.0	84.5 ± 4.4	205 ± 22.9	71.8 ± 2.7	443 ± 50.0	156 ± 6.2	345 ± 8.6	1171 ± 85.3
	CV	7.68	5.20	11.16	3.78	11.29	3.95	2.50	7.28
2016.1	Min	13.5	93.6	278	70.3	597	173	362	1408
	Max	16.2	118.0	317	81.2	776	200	414	1718
	Mean ± SD	14.5 ± 0.8	105.0 ± 8.87	293 ± 16.1	75.1 ± 3.7	683 ± 69.4	183 ± 8.1	395 ± 15.9	1563 ± 101.7
	CV	5.51	8.45	5.49	4.89	10.16	4.41	4.04	6.51
2017.12	Min	8.2	56.3	162	35.1	264	119	279	909
	Max	12.5	122.0	413	59.6	636	217	446	1545
	Mean ± SD	10.3 ± 0.9	79.5 ± 9.7	260 ± 21.7	46.7 ± 2.7	411 ± 75.3	159 ± 9.4	359 ± 11.3	1147 ± 183.7
	CV	8.74	12.20	8.35	5.78	18.3	5.91	3.15	16.02
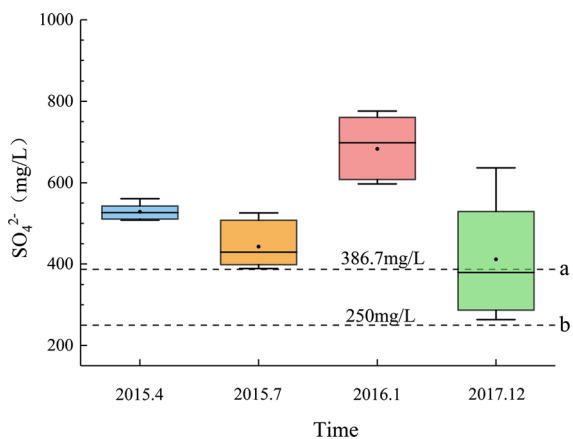
Fig. 2 Time variation in the sulfate of surface water in the Linhuan mining area **a** indicates the average value of SO_4^{2-} of the river water from the Huaibei coalfield and **b** indicates the standard limits for sulfate in drinking water set by the Environmental Quality Standard for Surface Water. Date from Chen et al. (2016)
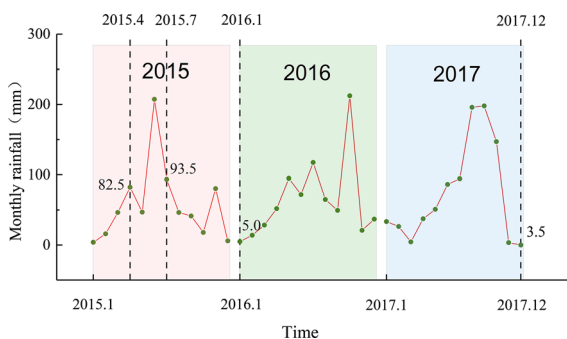

Fig. 3 Relationship between atmospheric precipitation and time in the Linhuan mining area (Data taken from published meteorological data)

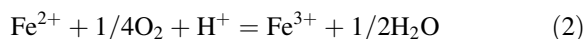Analysis of the sulfate sources in the mine drainage

Coal mining activities often produce a large amount of gangue, and the sulfur in gangue is mainly found in the form of pyrite. On the other hand, the environment caused by the destruction of strata by coal mining activities was beneficial to the oxidation of pyrite in the coal gangue and the production of a large amount of sulfate into the water body. The mine drainage and coal gangue samples were collected in Linhuan coal mine, and the water chemical indexes and isotopes of the samples were tested and analyzed. The results showed that the mine drainage was characterized by a high SO_4^{2-} concentration and high TDS. The average SO_4^{2-} and TDS contents reached 1270 ± 15.1 mg/L

and 2698 ± 35.3 mg/L, respectively, which indicated high salinity water. The mechanism of the high SO_4^{2-} content could be explored by testing the sulfur and oxygen isotopes of the sulfate in mine drainage. Coal mining activities also create conditions for the oxidation of pyrite. There are two reaction pathways by which pyrite oxidation produces sulfate in mine drainage systems (Fowler et al. 1999; Taylor et al. 1984).

In the first reaction, pyrite is mainly oxidized with O_2 as an oxidant when the pH is greater than 4.5:

$$FeS_2 + 7/2O_2 + H_2O = Fe^{2+} + 2H^+ + 2SO_4^{2-} \quad (1)$$
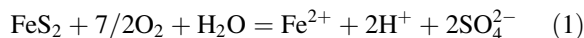
In the second reaction, pyrite is mainly oxidized by Fe^{3+} to an oxidant when the pH is less than 4.5 (Nordstrom et al. 1982):

$$Fe^{2+} + 1/4O_2 + H^+ = Fe^{3+} + 1/2H_2O \quad (2)$$

$$FeS_2 + 14Fe^{3+} + 8O_2 = 15Fe^{2+} + 16H^+ + 2SO_4^{2-} \quad (3)$$
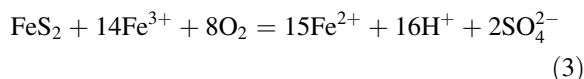
Under aerobic conditions, the oxidation of pyrite mainly occurs through the first reaction pathway. The second reaction route has multiple steps. In reaction (3), pyrite can be oxidized by Fe^{3+} to form SO_4^{2-} in an aerobic or anaerobic environment, and the reaction (2) occurs under aerobic conditions. In reaction (2), Fe^{2+} is oxidized as an intermediate product to Fe^{3+} to continue to participate in the oxidation of pyrite under aerobic conditions. The Fe ion concentration and pH in the mine drainage were tested. The Fe ion contents were 4.2 mg/L and 3.9 mg/L, and the pH values were 8.74 and 8.73. Based on further analysis of the Fe ion content, the high content of SO_4^{2-} in the mine drainage might be partly derived from the oxidation of pyrite, and the alkaline environment was conducive to the reaction of pyrite in the first oxidation route. Sulfide oxidation was mainly controlled by the formation rate of intermediate compounds of H_2O and O_2; therefore, the oxidation rate was faster. Under the condition of low temperature, the kinetic fractionation caused by the oxidation of sulfide was small, and the fractionation coefficients were close to 1. Experimental studies have shown that the sulfur isotope composition of SO_4^{2-} obtained by the oxidation of sulfide minerals is very close to its precursor sulfide minerals, and thus, the SO_4^{2-} generated by pyrite oxidation is basically the same as the $\delta^{34}S$ value of

sulfur (Sun et al. 2017; Liu et al. 2017). The pyrite δ^{34}S values of the collected gangue samples in the study area were 3.5‰ and 6.3‰, respectively, with an average of 4.9‰, while the δ^{34}S$_{SO4}$ values of SO_4^{2-} in the mine drainage were 26.8‰ and 26.7‰, with an average of 26.7‰. The δ^{34}S$_{SO4}$ value of SO_4^{2-} in the mine drainage was significantly higher than that of pyrite. There was a relatively obvious isotope enrichment phenomenon that did not conform to the sulfur isotope fractionation characteristics of sulfide oxidation, indicating that the sulfate generated by pyrite oxidation was not the main source of sulfate in the mine drainage. On the other hand, the positive δ^{34}S$_{SO4}$ value of SO_4^{2-} in the mine drainage was within the range of the sulfate isotope characteristic value of the dissolution of evaporate. However, the heavy isotope was enriched in the process of dissolution of the evaporite rock, giving priority to gypsum. The study found that the coal-bearing strata in Linhuan mining area consist of sandstone layer and siltstone layer, including quartz, feldspar, mica, gypsum and other minerals, including three groups of related coal seams, 7–8 coal seams, 10 coal seams (Wang et al. 2019; Chen et al. 2014,2017; Lin et al. 2016; Guo et al 2014). Therefore, the SO_4^{2-} in the mine drainage mainly originated from the dissolution of evaporite formation in the deep coal seam.

Above all, based on the Fe content and the isotopic characteristic value of SO_4^{2-} in the mine drainage, the high concentration of SO_4^{2-} in the mine drainage mainly originated from the dissolution of evaporite in the stratum, and the sulfate generated by the oxidation of pyrite was only a secondary source.

The difference was that, in general, the sulfate formed by sulfide oxidation was often enriched with light isotopes, and its δ^{34}S$_{SO4}$ value was usually negative. However, the Linhuan mining area showed a positive δ^{34}S$_{SO4}$ value, and the δ^{34}S value of the pyrite was different from that of the region. This regional differentiation phenomenon might be related to its unique coal-forming environment and the fractionation mechanism of isotopes in the oxidation process. Some scholars proposed a "north–south differentiation theory" (Hong et al. 1992). The sulfur in coal and coal gangue is mainly in the form of pyrite, and the sulfur isotopic composition of fossil fuels in different regions varies greatly due to their different geological backgrounds. Their sulfur isotopic compositions are quite different. By testing the sulfur isotope composition of coal mines in different regions of China, it was found that northern coal is characterized by a relatively high δ^{34}S value and a low sulfur content, while the southern coal is characterized by a relatively low δ^{34}S value and a high sulfur content. The difference in δ^{34}S values in the coals in the north and south could explain the phenomenon that the positive δ^{34}S$_{SO4}$ values of mine drainage and δ^{34}S values of pyrite in the study area showed a positive difference compared to other areas.

Isotope mixing model of surface water sulfate

The surface water composition in the mining area is mainly river water and subsidence area water. The sulfur and oxygen contents in the sulfate and the hydrogen and oxygen isotopes in the water are shown in Table 2. The sources of sulfate in surface waters are complex and can be divided into two categories: natural sources and anthropogenic sources. The natural sources of sulfate mainly include: the dissolution of evaporite rock, giving priority to gypsum, the oxidation of sulfide minerals (pyrite) and biological sulfur and the atmospheric acid deposition. The anthropogenic sources of sulfate mainly include: the discharge of industrial and domestic sewage, the use of agricultural fertilizer and coal mining activities. Except for the reduction in sulfate bacteria, sulfate in nature does not produce significant isotope fractionation, and there are some differences in the isotopic compositional characterization values of sulfates from different sources. Previously, the dissolution of evaporite rocks (such as gypsum) is often enriched with heavy isotopes, and their δ^{34}S value ranges from + 12‰ to + 35‰, and the eigenvalue of δ^{18}O$_{SO4}$ is + 6‰ to + 20‰. Atmospheric precipitation and sulfide oxidation and so on are often enriched with light isotopes. The δ^{34}S value of sulfide mineral oxidation ranged from − 5‰ to + 12‰, and the δ^{18}O$_{SO4}$ value ranged from − 5‰ to + 4‰ (Li et al. 2013; Balci et al. 2012; Baldwin and Mitchell 2012; Brunner et al. 2005). Therefore, the sulfate source could be analyzed based on the sulfate isotope characteristic value of the sample.

The isotope distribution of surface water in the mining area is shown in Fig. 4, the water sample points in the river, and the subsidence area all fell into the range of evaporite rocks. This result indicates that the sulfate source was mainly affected by evaporite

Table 2 Isotopic composition of the different types of surface water in the Linhuan mining area

Sampling no	$\delta^{34}S_{SO4}$ (‰ vs.VCDT)	$\delta^{18}O_{SO4}$ (‰ vs.VSMOW)	δD (‰ vs.VSMOW)	$\delta^{18}O_{H2O}$ (‰ vs.VSMOW)
Huihe River water				
HZ01	18.5	10.0	− 51.9	− 7.0
HZ02	18.2	9.3	− 51.8	− 6.9
XSG01	19.1	10.6	− 52.0	− 6.9
Mean ± SD	18.6 ± 0.4	10.0 ± 0.5	− 51.9 ± 0.08	− 6.9 ± 0.05
CV	2.01	5.33	0.16	0.68
Subsidence area water				
LHCX-01	21.3	11.9	− 42.0	− 5.1
LHCX-02	20.9	10.6	− 40.0	− 4.6
LHCX-03	20.2	10.9	− 47.6	− 6.0
LHCX-04	20.1	11.2	− 46.2	− 5.7
LHCX-05	21.6	10.0	− 29.3	− 2.6
LHCX-06	22.3	13.3	− 43.2	− 5.3
LHCX-07	20.8	10.8	− 40.8	− 4.7
LHCX-08	21.5	11.2	− 43.0	− 4.9
LHCX-09	20.9	11.3	− 43.4	− 5.2
LHCX-10	21.3	11.3	− 48.2	− 6.1
LHCX-11	21.4	11.1	− 41.2	− 4.8
LHCX-12	21.7	10.9	− 48.6	− 6.0
Mean ± SD	21.2 ± 0.6	11.2 ± 0.8	− 42.8 ± 5.0	− 5.1 ± 0.9
CV	2.83	6.85	11.59	17.79
Mine drainage				
LHK01	26.8	10.3	− 63.5	− 8.8
LHK02	26.7	10.3	− 65.7	− 8.9
Mean ± SD	26.8 ± 0.1	10.3 ± 0.0	− 64.6 ± 1.1	− 8.9 ± 0.1
CV	0.19	0.00	1.70	0.56
Atmospheric precipitation				
JS01	6.5	9.8	− 175.5	− 22.7
JS02	8.7	11.5	− 120.5	− 16.6
Mean ± SD	7.6 ± 1.1	10.7 ± 0.9	− 148.0 ± 27.5	− 19.7 ± 3.1
CV	14.47	7.98	18.58	15.52

dissolution. Based on previous studies, there is no obvious hydraulic connection between the surface water and groundwater in the study area, and the low SO_4^{2-} content in the groundwater had a weak influence on the water quality of the subsidence area. The subsidence area was formed by mining; the area connected with the Huihe River only by a gully and introduced river water is its water supply. Therefore, the SO_4^{2-} in the subsidence area water was mainly affected by river water. The range in the $\delta^{34}S_{SO4}$ value of SO_4^{2-} of the subsidence area was

+ 20.1‰ ∼ + 22.3‰, with an average of + 21.2 ± 0.6‰, while the range in the $\delta^{34}S_{SO4}$ value of SO_4^{2-} of the river was + 18.5‰ ∼ + 19.1‰, with an average of + 18.6 ± 0.4‰. There was an obvious isotope enrichment phenomenon in the SO_4^{2-} in the subsidence area, and the increase in the $\delta^{34}S_{SO4}$ value in the subsidence area indicated that there was a new pollution source in addition to the sulfate carried by the Huihe River. The average values of sulfate $\delta^{34}S_{SO4}$ and $\delta^{18}O_{SO4}$ of the mine drainage generated by mining in the surrounding subsidence area were +
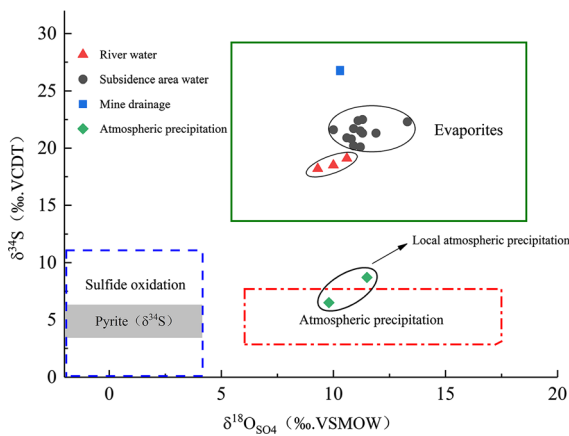
Fig. 4 Composition of $\delta^{34}S_{SO4}$ and $\delta^{18}O_{SO4}$ in the surface water in the Linhuan mining area and the isotope variation in the typical sulfate sources (pyrite $\delta^{34}S = 3.5‰$ and $6.3‰$). (1) Sulfate from evaporative rock: $\delta^{34}S_{SO4} = +12‰$ to $+35‰$, $\delta^{18}O_{SO4} = +6‰$ to $+20‰$. (2) Sulfate from oxidized sulfide: $\delta^{34}S_{SO4} = -18‰$ to $+12‰$, $\delta^{18}O_{SO4} = -5‰$ to $+5‰$. (3) Sulfate from atmospheric precipitation: $\delta^{34}S_{SO4} = -5‰$ to $+6‰$, $\delta^{18}O_{SO4} = +6‰$ to $+18‰$ (Based on Li et al. 2013)

$26.8 \pm 0.1‰$ and $+10.3 \pm 0.0‰$, respectively. The average of the $\delta^{34}S_{SO4}$ value in the subsidence area water was between the value of the Huihe River water and the value of the mine drainage. The high $\delta^{34}S_{SO4}$ value of the mining wastewater entering the subsidence zone caused the sulfate concentration and isotopic composition to change, which increased the $\delta^{34}S_{SO4}$ value of the water body. Considering that the possibility of sulfate reduction by bacteria (BSR) was small, it is possible that mine drainage was an important sulfate contributor. The average SO_4^{2-} concentration of the subsidence area water (490.6 ± 32.4 mg/L) was significantly higher than the average SO_4^{2-} concentration of the river water (279.1 ± 19.1 mg/L); this also verified this view. Similarly, the $\delta^{34}S_{SO4}$ and $\delta^{18}O_{SO4}$ values of the subsidence area water were obviously different from those of the local precipitation, and the average concentration of SO_4^{2-} in the precipitation was 13.8 ± 0.2 mg/L. The low concentration of SO_4^{2-} indicated that precipitation was not the main source of sulfate in the subsidence area water. In summary, the positive $\delta^{34}S_{SO4}$ value of sulfate in the river water was derived from the dissolution of evaporite in the upstream area, and the sulfate in the subsidence area water was derived from the recharge of river water and the influence of mining activities.

The result showed that the main sources of sulfates in the water bodies were quite different due to different geological backgrounds, rock mineral differences and human activities upstream of the different regions. The values of sulfate $\delta^{34}S_{SO4}$ in rivers and lakes in different regions of the world vary, and these differences are of great significance for the study of the conversion of sulfate sources and sulfur cycle transformation in regional waters (Li et al. 2013; Balci et al. 2007, 2012; Choi et al. 2011; Otero et al. 2008).

Since the sulfur isotope had no obvious isotope fractionation except for the reduction in sulfate bacteria, the reduction in sulfate bacteria in shallow lakes was not strong. Therefore, the isotope mass balance mixing model could be used to determine the source load ratio of sulfate. The three-terminal mixed model of the sulfur and oxygen isotope composition of sulfate in the study area is shown in Fig. 5. Except the samples (LHCX-05), most of the samples were in the triangle region proved the correctness of the model, which quantified the contribution proportion of the three pollution terminal sources. Because the main water body of the study was the subsidence area water, most of the water samples were mixed water samples or intermediate water samples. Recognizing the different end sources of sulfate recharge in the water body involved identifying the end sources based on the inversion of these intermediate samples. Some of the samples themselves were end source water (river water and mine drainage), determining the other end sources required combining the distributions of the
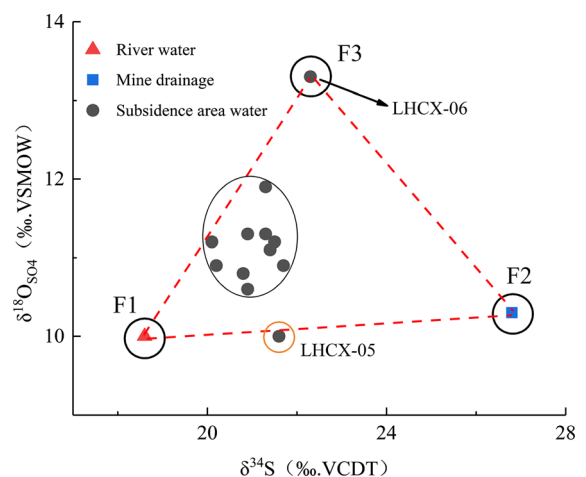

Fig. 5 Ternary mixing model of the sulfur and oxygen isotopes of the surface water in the Linhuan mining area

intermediate water samples. Among them, F1 represented the sulfate contribution proportion of the Huihe River water to the subsidence area water, and F2 represented the sulfate contribution proportion of mine drainage to the subsidence area water. End source F3 came from water sample (LHCX-06). There were a large number of coal gangue piles around the subsidence area due to coal mining activities. These gangues entered the subsidence area through surface runoff under the scouring action of rain water. Water sample (LHCX-06) was taken near the largest gangue pile in the subsidence water area. In Fig. 5, the isotope composition distribution of this point was obviously different from that of the other sampling points. The isotope composition of that water sample might be due to atmospheric precipitation mixed with the gangue leachate. The specific calculation formula of the ternary mixed model is as follows:

$$\delta^{34}S_1 \times F1 + \delta^{34}S_2 \times F2 + \delta^{34}S_3 \times F3 = \delta^{34}S_{MIX} \tag{4}$$

$$\delta^{18}O_1 \times F1 + \delta^{18}O_2 \times F2 + \delta^{18}O_3 \times F3 = \delta^{18}O_{MIX} \tag{5}$$

$$F1 + F2 + F3 = 1 \tag{6}$$

From Fig. 5, there was no relatively independent accumulation area of the water sample points in the subsidence area, and the difference in the end source points was also obvious. The value of $\delta^{34}S_{SO4}$ of the river terminal source (F1) was + 18.6‰, and the value of $\delta^{18}O_{SO4}$ was + 10.0‰; the value of $\delta^{34}S_{SO4}$ of the mine drainage (F2) was + 26.8‰, and the value of $\delta^{18}O_{SO4}$ was + 10.3‰; the value of $\delta^{34}S_{SO4}$ of the gangue leaching end source (F3) was + 22.3‰, and the value of $\delta^{18}O_{SO4}$ was + 13.3‰. Using these values in Eqs. (4) and (5), the specific calculation result of the source contribution ratio of each end source is shown in Fig. 6. The results showed that the sulfate contribution proportion of the river water source to the subsidence area water was 35.8–65.9%; the sulfate contribution proportion of the mine drainage source to the subsidence area water was 2.0–26.6%; and the sulfate contribution proportion of the gangue leaching end source ranged from 16.3 to 56.9%. The different water sample points were affected by different degrees of mine drainage and gangue leachate. The influence of coal mining
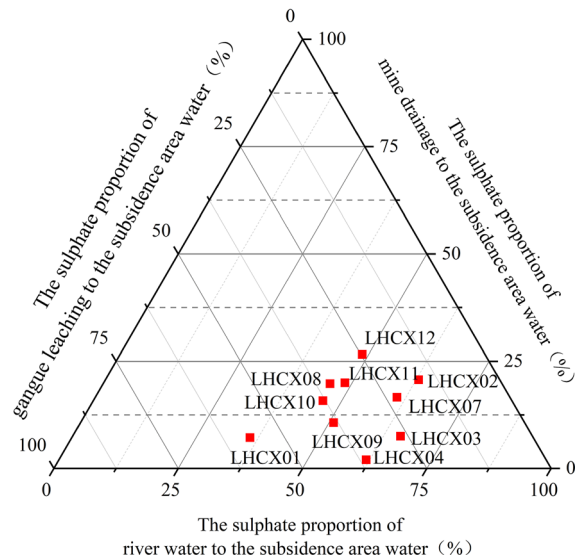

Fig. 6 The contribution of different end sources to the contribution of sulfate in the subsidence area

activities was the source of both mine drainage and gangue leaching. Therefore, the isotope mixing model accurately reflected the degree of influence of coal mining activities on the sulfate in the subsided area water.

The different points showed the difference in each pollution source in the study area and could reflect the different dominant sources of pollution at specific location. These results could be used to reduce environmental pollution due to the active transformation of mining areas, strengthen the follow-up treatment of mine wastewater and provide a reference for the rational selection of gangue accumulation locations. In addition, the high concentrations of sulfate in the surface water and mine drainage might infiltrate the groundwater and change its composition. Determining the sources and material circulation of groundwater hydrochemical components based only on different types of rock weathering and evaporation is problematic. Based on the combination of surface water characteristics and special pollutants, this study provides a basis for future research on groundwater in mining areas.

Conclusions

In this study area, the content of SO_4^{2-} in the surface water changed over time, and the value was higher than the average value of the "Environmental Quality Standard for Surface Water" (GB3838-2002). The content showed obvious seasonal variation in the high-flow, mid-flow and low-flow seasons, and sulfate pollution was serious. The sulfur and oxygen isotope compositions of the mine drainage were obviously enriched in heavy isotopes, the source of sulfate was mainly the dissolution of evaporative salt rocks in stratum, and pyrite oxidation was the secondary source. The main source of SO_4^{2-} in the river water was the dissolution of evaporite in the study area. The end source contributing SO_4^{2-} in the subsidence area were mainly river water, mine drainage and gangue leaching. The isotope ternary mixture was calculated by an isotope ternary mixed model. The proportion of sulfate contribution in the water ranged from 35.8 to 65.9%; the contribution of mine drainage source to the sulfate in the subsided water in the subsidence area ranged from 2.0 to 26.6%; the end source contribution of gangue leaching solution accounted for 16.3% to 56.9%. The results reflected that coal mining activities had an important impact on the concentration of sulfate in the subsidence area water.

The use of hydrochemistry and multi-isotopes ($\delta^{18}O_{SO4}$, $\delta^{34}S_{SO4}$) can accurately determine the source and contribution of SO_4^{2-} in surface water in the study area. The methodology here presented can be transferred to other sites and may provide a reliable base for the development of effective mitigation and adaptation strategies for sulfate pollution.

References

Balci, N., Mayer, B., Shanks, W. C., III, & Mandernack, K. W. (2012). Oxygen and sulfur isotope systematics of sulfate produced during abiotic and bacterial oxidation of sphalerite and elemental sulfur. *Geochimica et Cosmochimica Acta, 77*, 335–351.

Balci, N., Shanks, W. C., Mayer, B., & Mandernack, K. W. (2007). Oxygen and sulfur isotope systematics of sulfate produced by bacterial and abiotic oxidation of pyrite. *Geochimica et Cosmochimica Acta, 71*, 3796–3811.

Baldwin, D. S., & Mitchell, A. (2012). Impact of sulfate pollution on anaerobic biogeochemical cycles in a wetland sediment. *Water Research, 46*(4), 965–974.

Bao, H. (2006). Purifying barite for oxygen isotope measurement by dissolution and reprecipitation in a chelating solution. *Analytical Chemistry, 78*(1), 304–309.

Brunner, B., Bernasconi, S. M., Kleikemper, J., & Schroth, M. H. (2005). A model for oxygen and sulfur isotope fractionation in sulfate during bacterial sulfate reduction processes. *Geochimica et Cosmochimica Acta, 69*(20), 4773–4785.

Calmels, D., Jérôme, G., Agnès, B., & France-Lanord, C. (2007). Sustained sulfide oxidation by physical erosion processes in the Mackenzie River basin: Climatic perspectives. *Geology, 35*(11), 1003–1006.

Cao, X., Wu, P., Zhou, S., Sun, J., & Han, Z. (2018). Tracing the origin and geochemical processes of dissolved sulphate in a karst-dominated wetland catchment using stable isotope indicators. *Journal of Hydrology, 562*, 210–222.

Chen, G. Z., Wang, X. M., & Ru, W. (2019). Health risk assessment of potentially harmful elements in subsidence water bodies using a Monte Carlo approach: An example from the Huainan coal mining area, China. *Ecotoxicology and Environmental Safety, 171*, 737–745.

Chen, J., Liu, G. J., Jiang, M. M., Chou, C. L., Li, H., Wu, B., et al. (2011). Geochemistry of environmentally sensitive trace elements in Permian coals from the Huainan coalfield, Anhui China. *International Journal of Coal Geology, 88*(1), 41–54.

Chen, L. W., Xie, W. P., Feng, X. Q., Zhang, N. Q., & Yin, X. X. (2017). Formation of hydrochemical composition and spatio-temporal evolution mechanism under mining-induced disturbance in the Linhuan coal-mining district. *Arabian Journal of Geosciences, 10*(3), 1–13.

Chen, L. W., Yin, X. X., Xie, W. P., & Feng, X. Q. (2014). Calculating groundwater mixing ratios in groundwater-inrushing aquifers based on environmental stable isotopes (D, ^{18}O) and hydrogeochemistry. *Natural Hazards, 71*, 937–953.

Chen, S., & Gui, H. R. (2016). Chemical characteristics of river water in Huaibei Coalfield, China and its significance. *Earth and Environment, 44*(4), 414–421.

Choi, B. Y., Yun, S. T., Mayer, B., & Kim, K. H. (2011). Sources and biogeochemical behavior of nitrate and sulfate in an alluvial aquifer: Hydrochemical and stable isotope approaches. *Applied Geochemistry, 26*(7), 1249–1260.

Dogramaci, S. S., Herczeg, A. L., Schiff, S. L., & Bone, Y. (2001). Controls on $\delta^{34}S$ and $\delta^{18}O$ of dissolved sulfate in aquifers of the Murray Basin, Australia and their use as indicators of flow processes. *Applied Geochemistry, 16*(4), 475–488.

Fan, Y., Li, H., Xue, Z., Zhang, Q., & Cheng, F. (2017). Accumulation characteristics and potential risk of heavy metals in soil-vegetable system under greenhouse

cultivation condition in northern China. *Ecological Engineering*, *102*, 367–373.

Fang, T., Liu, G. J., Zhou, C. C., & Lu, L. L. (2015). Lead in soil and agricultural products in the Huainan coal mining area, Anhui, China: Levels, distribution, and health implications. *Environmental Monitoring and Assessment*, *187*(3), 152–162.

Fowler, T. A., Holmes, P. R., & Crundwell, F. K. (1999). Mechanism of pyrite dissolution in the presence ofThiobacillus Ferrooxidans. *Applied and Environmental Microbiology*, *65*(7), 2987–2993.

Guo, P. K., Cheng, Y. P., Jin, K., & Liu, Y. P. (2014). The impact of faults on the occurrence of coal bed methane in Renlou coal mine, Huaibei coalfield, China. *Journal of Natural Gas Science and Engineering*, *17*, 151–158.

Han, F., & Zhang, Y. (2017). Distribution characteristic and migration pathways of metals in subsidence zone in a coal mine, China. *Bulletin of Environmental Contamination and Toxicology*, *98*(4), 539–545.

Hong, Y. T., Zhang, H. B., & Zhu, Y. X. (1992). Sulfur isotope composition characteristics of coal in China and sulfur isotope fractionation in coal combustion process. *Chinese Science*, *8*, 868–873.

Hu, Y., Dong, Z., & Liu, G. J. (2017). Distribution and potential ecological risk of heavy metals accumulated in subsidence lakes formed in the Huainan coalfield China. *Environmental Forensics*, *18*(4), 251–257.

Li, X., Gan, Y., Zhou, A., & Liu, Y. (2015). Relationship between water discharge and sulfate sources of the Yangtze River inferred from seasonal variations of sulfur and oxygen isotopic compositions. *Journal of Geochemical Exploration*, *153*, 30–39.

Li, X., Gan, Y., Zhou, A., Liu, Y., & Wang, D. (2013). Hydrological controls on the sources of dissolved sulfate in the Heihe River, a large inland river in the arid northwestern China, inferred from S and O isotopes. *Applied Geochemistry*, *35*(4), 99–109.

Lin, M. L., Peng, W. H., & Gui, H. R. (2016). Hydrochemical characteristics and quality assessment of deep groundwater from the coal-bearing aquifer of the Linhuan coal-mining district, Northern Anhui Province, China. *Environmental Monitoring and Assessment*, *188*(4), 202–215.

Liu, M., Guo, Q., Zhang, C., Zhu, M., & Li, J. (2017). Sulfur isotope geochemistry indicating the source of dissolved sulfate in Gonghe geothermal waters, northwestern China. *Procedia Earth and Planetary Science*, *17*, 157–160.

Liu, J. S., Yan, J. P., Xu, L. J., Gu, B., & Zhang, L. (2009). Water environment in different subsidence pools of Huainan coal-mining area: Investigation and evaluation. *Environmental Science Technology*, *32*(9), 140–143. **(in Chinese)**.

Lu, L., Liu, G., Wang, J., & Liu, Y. (2017a). Accumulation and health risk assessment of trace elements in Carassius auratus gibelio from subsidence pools in the Huainan coalfield in China. *Environmental Monitoring and Assessment*, *189*(9), 479–483.

Lu, L., Liu, G., Wang, J., & Wu, Y. (2017b). Bioavailability and mobility of heavy metals in soil in vicinity of a coal mine from Huaibei, China. *Human and Ecological Risk Assessment: An International Journal*, *23*(5), 1164–1177.

Nordstrom, D. K. (1982). Aqueous pyrite oxidation and the consequent formation of secondary iron minerals. *Acid Sulfate Weathering Soil Science Society of America*, *10*, 37–56.

Nriagu, J. O., Rees, C., Mekhtiyeva, V., Lein, A. Y., & Krouse, H. R. (1991). Hydrosphere. Stable isotopes: Natural and anthropogenic sulphur in the environment. *Scope*, *43*, 177–265.

Otero, N., Soler, A., & Canals, À. (2008). Controls of δ^{34}S and δ^{18}O in dissolved sulphate: Learning from a detailed survey in the Llobregat River (Spain). *Applied Geochemistry*, *23*, 1166–1185.

Qiu, H., Gui, H., & Song, Q. (2018). Human health risk assessment of trace elements in shallow groundwater of the Linhuan coal-mining district, northern Anhui province, China. *Ecological Risk Assessment: An International Journal*, *24*(5), 1342–1351.

Shang, W. Q., Tang, Q., Zheng, L. G., & Cheng, H. (2016). Chemical forms of heavy metals in agricultural soils affected by coal mining in the Linhuan subsidence of Huaibei coalfield, Anhui province, China. *Environmental Science and Pollution Research*, *23*(23), 23683–23693.

Sun, J., Kobayashi, T., Strosnider, W. H. J., & Wu, P. (2017). Stable sulfur and oxygen isotopes as geochemical tracers of sulfate in karst waters. *Journal of Hydrology*, *551*, 245–252.

Taylor, B. E., Wheeler, M. C., & Nordstrom, D. K. (1984). Isotope composition of sulphate in acid mine drainage as measure of bacterial oxidation. *Nature*, *308*(5959), 538–541.

Torssander, P., Morth, C. M., & Kumpulainen, R. (2006). Chemistry and sulfur isotope investigation of industrial wastewater contamination into groundwater aquifers, Pitea County N. Sweden. *Journal of Geochemical Exploration*, *88*(1–3), 60–67.

Wang, D., Tian, F., Yang, M., Liu, C., & Li, Y. F. (2009). Application of positive matrix factorization to identify potential sources of PAHs in soil of Dalian China. *Environmental Pollution*, *157*(5), 1559–1564.

Wang, M. C., Gui, H. R., & Hu, R. J. (2019). Hydrogeochemical characteristics and water quality evaluation of carboniferous Taiyuan formation limestone water in Sulin Mining Area in Northern Anhui, China. *International Journal of Environmental Research and Public Health*, *16*(2512), 1–14.

Wang, X. M., Chu, Z. X., Zha, F. G., Liu, S. M., Liu, G. J., & Dong, Z. B. (2015). Determination of heavy metals in water and tissues of Crucian Carp (Carassius auratus Gibelio) collected from subsidence pools in Huainan coal fields (China). *Analytical Letters*, *48*(5), 861–877.

Wei, Y., Fan, Z. J., Sun, L., & Liu, G. J. (2016). Study on sustainable utilization of water resources in coal mining subsidence area: a case study in Huainan City, China. *Journal of Minzu University of China (Natural Sciences Edition)*, *25*(4), 10–14.

Xie, K., Zhang, Y., Yi, Q., & Yan, J. (2013). Optimal resource utilization and ecological restoration of aquatic zones in the coal mining subsidence areas of the Huaibei plain in Anhui province, China. *Desalination & Water Treatment*, *51*(19–21), 4019–4027.

Yi, Q., Sun, P., Niu, S., & Kim, Y. (2015). Potential for sediment phosphorus release in coal mine subsidence lakes in China:

Perspectives from fractionation of phosphorous, iron and aluminum. *Biogeochemistry, 126*(3), 315–327.

Zhang, D., Huang, X. Y., & Li, C. J. (2013). Sources of riverine sulfate in Yellow River and its tributaries determined by sulfur and oxygen isotopes. *Advances in Water Science, 24*(3), 418–426.

Zhang, Q., Wang, F., & Chen, M. (2014). Study on wetland connectivity technology in the urban coalmine subsidence area of Huaibei China-hydrological guarantee analysis. *Wetlands, 34*(5), 841–852.

Zhang, R. Y., Xiao, W., Yang, J., Ren, J. T., Jiang, S., & Wang, P. F. (2015). Scenario analysis of mining subsidence in Huaibei city and governance patterns. In *Beijing international symposium on land reclamation and ecological restoration*.